Time evolution of relativistic d + Au and Au + Au collisions

Georg Wolschin[1], Minoru Biyajima[2],
Takuya Mizoguchi[3], and Naomichi Suzuki[4]

[1] Institut für Theoretische Physik der Universität, D-69120 Heidelberg, Germany
[2] Department of Physics, Shinshu University, Matsumoto 390-8621, Japan
[3] Toba National College of Maritime Technology, Toba 517-8501, Japan
[4] Department of Comprehensive Management,
Matsumoto University, Matsumoto 390-1295, Japan

The evolution of charged-particle production in collisions of heavy ions at relativistic energies is investigated as function of centrality in a nonequilibrium-statistical framework. Precise agreement with recent d + Au and Au + Au data at $\sqrt{s_{NN}} = 200$ GeV is found in a Relativistic Diffusion Model with three sources for particle production. Only the midrapidity source comes very close to local equilibrium, whereas the analyses of the overall pseudorapidity distributions show that the systems remain far from statistical equilibrium.

Key words Relativistic heavy-ion collisions, nonequilibrium-statistical approach, Relativistic Diffusion Model
PACS 25.75.-q, 24.60.Ky, 24.10.Jv, 05.40.-a

1 Introduction

The investigation of particle production in relativistic heavy-ion collisions at the highest available energies offers an ideal opportunity to study the gradual approach to statistical equilibrium in a strongly interacting many-particle system. It has recently been shown by several groups that analytically soluble non-equilibrium statistical models are suitable to accurately describe a fairly large amount of phenomena that are observed experimentally. This allows us to determine how closely the system approaches thermal equilibrium in the course of particle production during the collision.

In particular, pseudorapidity distributions of primary charged particles have become available [1] as functions of centrality in d + Au collisions at a nucleon-nucleon center-of-mass energy of 200 GeV. They complement corresponding data on particle production for the heavy Au + Au system at various incident energies [2, 3]. Both are investigated within a nonequilibrium-statistical framework that is based on analytical solutions of a Relativistic Diffusion Model (RDM).

We investigate these solutions as functions of time for both asymmetric, and symmetric systems in comparison with the data. Whereas the midrapidity source for particle production comes very close to equilibrium in rapidity space, this is not the case for the target- and projectile-like sources. They remain far from equilibrium, and produce the characteristic nonequilibrium shape of the overall rapidity distribution function. This is particularly evident in case of the asymmetric d + Au system, where the steeper slope in the deuteron direction is shown to be an immediate consequence of the nonequilibrium properties. A short account of this work has been given in [4].

The analytical model is outlined in section 2. The time dependence of the solutions in pseudorapidity space, and the pseudorapidity distributions for produced charged hadrons as functions of collision centrality are obtained in section 3 for d + Au, and in section 4 for Au + Au. The conclusions are drawn in section 5.

2 Relativistic Diffusion Model

Nonequilibrium processes such as those observed in the course of particle production during relativistic heavy-ion collisions have successfully been described in many areas of physics by Fokker-Planck equations (FPEs) [5, 6]. These were also used in Brownian motion of macroscopic particles in a heat bath [7, 8, 9], where they allow to model both the velocity- and the spatial distribution of test particles. Due to the large number of produced particles in relativistic heavy-ion collisions and the random nature of their mutual strong interactions [10], such equations are useful in the detailed modelling of the distribution functions even though there is no heat bath present. However, Lorentz-invariant kinematical variables have to be introduced. In particular, the rapidity replaces the velocity to describe the motion parallel to the beam direction, and for the transverse motion a corresponding transverse rapidity may be introduced.

In this work we concentrate on the ordinary (longitudinal) rapidity. The analysis will show that thermal equilibrium is not reached in particle production, but one comes sufficiently close to it to justify the use of the FPE. The present investigation is based on a linear Fokker-Planck equation for three components $R_k(y,t)$ of the distribution function for produced charged hadrons in rapidity space [11, 12, 13]

$$\frac{\partial}{\partial t}R_k(y,t) = \frac{1}{\tau_y}\frac{\partial}{\partial y}\Big[(y-y_{eq})\cdot R_k(y,t)\Big] + \frac{\partial^2}{\partial^2 y}\Big[D_y^k \cdot R_k(y,t)\Big] \tag{1}$$

with the rapidity $y = 0.5 \cdot ln((E+p)/(E-p))$. The diagonal components D_y^k of the diffusion tensor contain the microscopic physics in the respective target-like (k=1), projectile-like (k=2) and central (k=3) regions. They account for the broadening of the distribution functions through interactions and particle creations. In the present investigation the off-diagonal terms of the diffusion tensor are assumed to be zero. The rapidity relaxation time τ_y determines the speed of the statistical equilibration in y-space.

As time goes to infinity, the mean values of the solutions of Eqs. (1) approach the equilibrium value y_{eq}. We determine it from energy- and momentum conservation [14, 15] in the system of target- and projectile-participants and hence, it depends on impact parameter. This dependence is decisive for a detailed description of the measured charged-particle distributions in asymmetric systems:

$$y_{eq}(b) = 1/2 \cdot ln \frac{< m_1^T(b) > exp(y_{max}) + < m_2^T(b) > exp(-y_{max})}{< m_2^T(b) > exp(y_{max}) + < m_1^T(b) > exp(-y_{max})} \tag{2}$$

with the beam rapidities $y_b = \pm y_{max}$, the transverse masses $< m_{1,2}^T(b) >= \sqrt{(m_{1,2}^2(b) + < p_T >^2)}$, and masses $m_{1,2}(b)$ of the target- and projectile-like participants that depend on the impact parameter b. The average numbers of participants $< N_{1,2}(b) >$ in the incident nuclei are calculated from the geometrical overlap. The results are consistent with the Glauber calculations reported in [1] for d + Au and in [2] for Au + Au which we use in the further analysis.

The corresponding equilibrium values of the rapidity are zero in symmetric systems. In the asymmetric d + Au case, they vary from y_{eq} = - 0.169 for peripheral (80-100%) to y_{eq} = - 0.944 for central (0-20%) collisions. They are negative due to the net longitudinal momentum of the participants in the laboratory frame, and their absolute magnitudes decrease with increasing impact parameter since the number of participants decreases for more peripheral collisions.

The RDM describes the drift of the mean values of the partial distributions towards y_{eq}. The existence of this drift has clearly been established from the comparison of RDM-results with net-proton rapidity distributions at various incident energies [13], where it is directly visible in the available data from the NA 49 and BRAHMS collaborations. For produced hadrons, the drift of the partial distribution functions is not directly visible in the data, although its presence is essential for a precise modeling of the results.

Whether the mean values of the distribution functions R_1 and R_2 actually attain y_{eq} depends on the interaction time τ_{int} (the time the system interacts strongly, or the integration time of (1)). It can be determined from dynamical models or from parametrizations of two-particle correlation measurements. For central Au + Au at 200 A GeV, this yields about $\tau_{int} \simeq 10 fm/c$ [16], which is too short for R_1 and R_2 to reach equilibrium. Note, however, that this does not apply to R_{eq} which is born near local equilibrium at short times (in the present calculation, at t = 0 due to the $\delta-$function intitial conditions), and then spreads in time through diffusive interactions with other particles at nearly the same rapidity. Although its variance does not fully attain the thermal limit in the collisions investigated here, we refer to R_{eq} as the local equilibrium distribution since it comes very close to it.

Nonlinear effects are not considered here. These account to some extent for the collective expansion of the system in $y-$space, which is not included a priori in a statistical treatment. In the linear model, the expansion is treated through effective diffusion coefficients D_y^{eff} that are larger than the theoretical values calculated from the dissipation-fluctuation theorem that normally relates D_y and τ_y to each other [18]. One can then deduce the collective expansion velocities from a comparison between data and theoretical result.

The FPE can be solved analytically in the linear case with constant D_y^k. For net-baryon rapidity distributions, the initial conditions are δ-functions at the beam rapidities $y_b = \pm y_{max}$. However, it has been shown that in addition there exists a central (k=3, equilibrium) source at RHIC energies which accounts for about 14% of the net-proton yield in Au + Au collisions at 200 AGeV [13], and is most likely related to deconfinement. For d + Au, net-proton rapidity distributions are not yet available.

For produced particles, the initial conditions are not uniquely defined. Our previous experience with the Au + Au system regarding both net baryons [13], and produced hadrons [19] favors a three-sources approach, with δ-function initial conditions at the beam rapidities, supplemented by a source centered at the equilibrium value y_{eq}. This value is equal to zero for symmetric systems, but for the asymmetric d + Au case its deviation from zero according to (2) is decisive in the description of particle production.

Physically, the particles in this source are expected to be generated mostly from gluon-gluon collisions since only few valence quarks are present in the midrapidity region at $\sqrt{s_{NN}} = 200$ GeV [13]. Particle creation from a gluon-dominated source, in addition to the sources related to the valence part of the nucleons, has also been proposed by Bialas and Czyz [20]. The final width of this source corresponds to the local equilibrium temperature of the system which may approximately be obtained from analyses of particle abundance ratios, plus the broadening due to the collective expansion of the system. Formally, the local equilibrium distribution is a solution of (1) with diffusion coefficient $D_y^3 = D_y^{eq}$, and δ-function initial condition at the equilibrium value.

The PHOBOS-collaboration has analyzed their minimum-bias data successfully using a triple Gaussian fit [21]. This is consistent with our analytical three-sources approach, although additional contributions to particle production have been proposed. Beyond the precise representation of the data, however, the Relativistic Diffusion Model offers an analytical description of the statistical equilibration during the collision and in particular, of the extent of the moving midrapidity source which is indicative of a locally equilibrated parton plasma prior to hadronization.

With $\delta-$function initial conditions for the Au-like source (1), the d-like source (2) and the equilibrium source (eq), we obtain exact analytical diffusion-model solutions as an incoherent superposition of the distribution functions $R_k(y,t)$ because the differential equation is linear. The three individual distributions are Gaussians with mean values

$$< y_{1,2}(t) >= y_{eq}[1 - exp(-t/\tau_y)] \mp y_{max} \exp{(-t/\tau_y)} \tag{3}$$

for the sources (1) and (2), and y_{eq} for the moving equilibrium source. Hence, all three mean values attain $y_{eq}(b)$ as determined from (2) for t$\rightarrow \infty$, whereas for short times the mean rapidities are smaller than, but close to the Au- and d-like values in the sources 1 and 2. The variances are

$$\sigma^2_{1,2,eq}(t) = D_y^{1,2,eq}\tau_y[1 - \exp(-2t/\tau_y)]. \tag{4}$$

The charged-particle distribution in rapidity space is then obtained as incoherent superposition of nonequilibrium and local equilibrium solutions of (1)

$$\frac{dN_{ch}(y, t = \tau_{int})}{dy} = N^1_{ch}R_1(y, \tau_{int}) + N^2_{ch}R_2(y, \tau_{int}) + N^{eq}_{ch}R^{loc}_{eq}(y, \tau_{int}) \tag{5}$$

with the interaction time τ_{int} (total integration time of the differential equation), and the partial distributions (k=1,2,eq)

$$R_k(y, \tau_{int}) = \frac{1}{\sqrt(2\pi\sigma^2_k(\tau_{int}))} exp\Big[-\frac{(y- < y_k(\tau_{int}) >)^2}{2\sigma^2_k(\tau_{int})}\Big]. \tag{6}$$

The incoherent sum of these distributions differs decisively from a single Gaussian that is sometimes taken to model pseudorapiditry distributions for produced particles (together with the Jacobian transformation that would generate the dip seen in the data at midrapidity for symmetric systems, cf. sect.3).

In the present work, the integration is stopped at the value of τ_{int}/τ_y that produces the minimum χ^2 with respect to the data and hence, the explicit value of τ_{int} is not needed as an input. The result for central collisions is $\tau_{int}/\tau_y \simeq 0.4$ for d + Au, and $\tau_{int}/\tau_y \simeq 0.46$ for Au + Au. As the time evolution parameter in the actual numerical calculation we take $p = (1 - exp(-2t/\tau_y))$, and the corresponding values are p= 0.55 for d + Au, and 0.6 for Au + Au.

The average numbers of charged particles in the target- and projectile-like regions $N_{ch}^{1,2}$ are proportional to the respective numbers of participants $N_{1,2}$,

$$N_{ch}^{1,2} = N_{1,2}\frac{(N_{ch}^{tot} - N_{ch}^{eq})}{(N_1 + N_2)} \tag{7}$$

with the constraint $N_{ch}^{tot} = N_{ch}^{1} + N_{ch}^{2} + N_{ch}^{eq}$. Here the total number of charged particles in each centrality bin N_{ch}^{tot} is determined from the data. The average number of charged particles in the equilibrium source N_{ch}^{eq} is a free parameter that is optimized together with the variances and τ_{int}/τ_y in a χ^2-fit of the data using the CERN minuit-code [22]. With known τ_{int}, including its dependence on centrality, one could then determine τ_y and D_y, but this is beyond the scope of the present work.

3 Application to d + Au collisions

The time evolution of the resulting RDM-solutions is shown in Fig.1 for central collisions of d + Au at $\sqrt{s_{NN}} = 200$ GeV for short values of $\tau_{int}/\tau_y = 0.005$ (p=0.01), and large values $\tau_{int}/\tau_y = 2.3$ (p=0.99). In the latter case, the system is already very close to statistical equilibrium in pseudorapidity space, as is evident from the distribution functions shown in the lower part of Fig.1, which are almost symmetric with respect to the equilibrium value. In the actual collision, the system remains between these two extreme cases, and in particular, it remains far from the equilibrium situation, because strong interaction stops long before this situation is approached, see Fig.2.

We present the results in pseudorapidity space $\eta = -ln[tan(\theta/2)]$ since particle identification was not available. The conversion from $y-$ to $\eta-$ space of the rapidity density

$$\frac{dN}{d\eta} = \frac{dN}{dy}\frac{dy}{d\eta} = \frac{p}{E}\frac{dN}{dy} = J(\eta, \langle m\rangle/\langle p_T\rangle)\frac{dN}{dy} \tag{8}$$

is performed through the Jacobian

$$J(\eta, \langle m\rangle/\langle p_T\rangle) = \cosh(\eta) \cdot [1 + (\langle m\rangle/\langle p_T\rangle)^2 + \sinh^2(\eta)]^{-1/2}. \tag{9}$$

Here we approximate the average mass $< m >$ of produced charged hadrons in the central region by the pion mass m_π, and use a mean transverse momentum $< p_T > = 0.4$ GeV/c.

In the Au-like region, the average mass is larger due to the participant protons, but since their number $Z_1 < 5.41$ is small compared to the number of produced charged hadrons in the d + Au system, the increase above the pion mass remains small: $< m >\approx m_p \cdot Z_1/N^1_{ch} + m_\pi \cdot (N^1_{ch} - Z_1)/N^1_{ch} \approx 0.17 GeV$. This increase turns out to have a negligeable effect on the results of the numerical optimization, where we use $< m > / < p_T >= 0.45$ for the Jacobian transformations in the three regions. For reasonable deviations of the mean transverse momentum from 0.4 GeV/c, the results remain consistent with the data within the experimental error bars.

The result of the RDM calculation is shown in Fig. 2 for five collision centralities of d + Au, and minimum-bias, and compared to recent PHOBOS data [1, 21]. In case of central collisions, the charged-particle yield is dominated by hadrons produced from the Au-like source, but there is a sizeable equilibrium source that is more important than the d-like contribution. This thermalized source is moving since y_{eq} has a negative value for d + Au, whereas it is zero for symmetric systems.

The equilibrium source in the light and asymmetric d + Au system is found to contain only 19% of the produced charged hadrons in central collisions. The total particle number and the particles created from the Au-like source decrease almost linearly with increasing impact parameter, but the magnitude of the equilibrium source is found to be roughly independent of centrality [4]. As a consequence, particle production in the equilibrium source is relatively more important in peripheral collisions. The variance of the central source lies for sufficiently small impact parameters between the values for the Au- and d-like sources [4]. In the equilibrium source, a statistical descrition of particle production in terms of a temperature and a chemical potential is meaningful. This is, however, not the case for the nonequilibrium fractions of the distribution function.

The minimization procedure yields precise results so that reliable values for the relative importance of the three sources for particle production can be determined, Table 1. Here the average impact parameters $< b_j >$ for the five centrality cuts j are determined according to

$$< b_j >= \int b\sigma_j(b)db / \int \sigma_j(b)db \tag{10}$$

with the geometrical cross sections $\sigma_j(b)$. In a sharp-cutoff model with limiting impact parameters b_1, b_2 in each centrality bin j, this is

$$< b_j >= \frac{2}{3}\Big(\frac{b_2^3 - b_1^3}{b_2^2 - b_1^2}\Big)_j. \tag{11}$$

Whereas the total particle number and the particles created from the Au-like source decrease almost linearly with increasing impact parameter, the magnitude of the equilibrium source is roughly independent of centrality. As a consequence, particle production in the equilibrium source is relatively more important in peripheral collisions. The variance of the central source lies for sufficiently small impact parameters between the values for the Au- and d-like sources.

The rapidity relaxation times and diffusion coefficients can also be obtained from (3),(4), but this requires an independent information about the interaction times. A small discrepancy in case of the most peripheral collisions (80-100%) is a consequence of the three straggling data points in the region -4 $< \eta < -3$.

The observed shift of the distributions towards the Au-like region in more central collisions, and the steeper slope in the deuteron direction as compared to the gold direction appear in the Relativistic Diffusion Model as a consequence of the gradual (incomplete) approach to equilibrium. The dependence of the shape and the absolute magnitudes on centrality are particularly evident in Fig.3 where the pseudorapidity distributions for all centralities are shown in a single plot in comparison with the PHOBOS data.

Given the structure of the underlying differential equation that we use to model the equilibration, together with the initial conditions and the constraints imposed by Eqs. (2) and (7), there is no room for substantial modifications of this result. In particular, changes in the impact-parameter dependence of the mean values in (3) that are not in accordance with (2) vitiate the precise agreement with the data.

4 Application to Au + Au

The three-sources RDM has previously been applied to the Au + Au system at various incident energies for net protons [13], and for produced charged hadrons [19]. For net protons, the number of particles contained in the midrapidity source can be determined rather accurately, whereas this is not the case for produced charged hadrons. This is due to the uncertainty in the initial conditions ($\delta-$functions are clearly correct for the participant protons, but they remain ambiguous for produced particles), and also due to the symmetry of the system, which does not permit unique results of a χ^2-fit of the data.

A previous result [19] for Au + Au in the three-sources-RDM shows indeed that the size of the equilibrium source for particle production at a given centrality can not be determined uniquely, and may be different in the heavy system [19] at the same energy as compared to d + Au. Here we fix the particle content in the midrapidity source at a given value of $< b > /b_{max}$ to approximately the same value as in the d + Au case, where the result is given from fitting the analytical solutions to the data (see Tab.1). Here $< b >$ is determined for a given centrality as described in the previous section.

The result for central Au + Au-collisions at $\sqrt{s_{NN}} = 200$ GeV is shown in Fig.4 (upper frame) together with PHOBOS data [3]. The time evolution of the RDM-solutions can be seen by comparing short-time solutions (middle frame for short values of $\tau_{int}/\tau_y = 0.005$, or p=0.01) with the solutions for large times (lower frame for $\tau_{int}/\tau_y = 2.3$, or p=0.99). In the latter case, the system is again very close to statistical equilibrium in pseudorapidity space. The actual collision with $\tau_{int}/\tau_y = 0.46$, or p=0.6, (top frame) remains between these two extreme cases.

The comparison with PHOBOS data for various centralities can be seen in Fig.5, where the individual partial distributions are also shown. For each centrality, the percentage of produced charged hadrons is taken approximately from the d + Au results. It rises for more peripheral collisions, because the number of charged hadrons produced from nucleon-nucleon collisions in the target- and projectile-like region of pseudorapidity space falls more strongly than the overall number of produced hadrons. However, the formation of an equilibrated quark-gluon plasma in the local equilibrium region prior to hadronization can probably only be expected for central collisions, since it requires high excitation and density.

5 Conclusion

To conclude, we have investigated charged-particle production in d + Au and Au + Au collisions at $\sqrt{s_{NN}}$= 200 GeV as function of centrality within the framework of an analytically soluble three-sources model. Excellent agreement with recent PHOBOS pseudorapidity distributions has been obtained, and from a χ^2-minimization we have determined the diffusion-model parameters very accurately.

For central d + Au collisions, a fraction of only 19% of the produced particles arises from the locally equilibrated midrapidity source. Although this fraction increases towards more peripheral collisions, the formation of a thermalized parton plasma prior to hadronization can probably only be expected for more central collisions.

The d + Au results show clearly that only the midrapidity part of the distribution function comes very close to thermal equilibrium, whereas the interaction time is too short for the d- and Au-like parts to attain the thermal limit. The same is true for the heavy Au + Au system at the same energy, but there the precise fraction of particles produced in the equilibrium source is more difficult to determine due to the symmetry of the problem.

The relativistic systems can thus be seen to be on their way towards statistical equilibrium. However, due to the dynamical evolution both the asymmetric and the symmetric system remain far from reaching thermodynamic equilibrium, which is closely approached only by the hadrons created from the central source that is mostly due to gluon-gluon collisions.

Acknowledgement One of the authors (GW) acknowledges the hospitality of the Faculty of Sciences at Shinshu University, and financial support by the Japan Society for the Promotion of Science (JSPS) which are due to contacts at RCNP (Osaka University) and the Yukawa Institute of Theoretical Physics (YITP) at Kyoto University.

References

[1] B.B. Back, et al., Phys. Rev. C **72**, 031901 (2005).

[2] B.B. Back, et al., nucl-ex/0509034, submitted to Phys. Rev. C.

[3] R. Nouicer et al., nucl-ex/0208003, Proc. XXXVII Rencontres de Moriond (2002).

[4] G. Wolschin, M. Biyajima, T. Mizoguchi, and N. Suzuki, Phys. Lett. B **633**, 38 (2006).

[5] A.D. Fokker, Ann. Phys. (Leipzig) **43**, 810 (1914); M. Planck, Sitzber. Preuß. Akad. Wiss. p. 324 (1917).

[6] N.G. van Kampen, Phys. Bl. **53**, 1012 (1997).

[7] Lord Rayleigh, Phil. Mag. **32**, 424 (1891).

[8] A. Einstein, Ann. Phys. (Leipzig) **17**, 549 (1905); **19**, 289 (1906); **19**, 371 (1906).

[9] G.E. Uhlenbeck and L.S. Ornstein, Phys. Rev. **36**, 823 (1930).

[10] I. Arsene et al., Nucl. Phys. A **757**, 1 (2005).

[11] G. Wolschin, Eur. Phys. J. A **5**, 85 (1999).

[12] M. Biyajima, M. Ide, T. Mizoguchi, and N. Suzuki, Prog. Theor. Phys. **108**, 559 (2002); **109**, 151 (2003).

[13] G. Wolschin, Phys. Lett. B **569**, 67 (2003); Phys. Rev. C **69**, 024906 (2004); hep-ph/0502123.

[14] H.J. Bhabha, Proc. Roy. Soc. (London) A **219**, 293 (1953).

[15] S. Nagamiya and M. Gyulassy, Adv. Nucl. Phys. **13**, 201 (1984).

[16] M. Lisa, S. Pratt, R. Soltz, and U. Wiedemann, Ann. Rev. Nucl. Part. Sci. **55**, 357 (2005).

[17] M. Rybczyński, Z. Włodarczyk, and G. Wilk, Nucl. Phys. B (Proc. Suppl.) **122**, 325 (2003).

[18] G. Wolschin, Europhys. Lett. **47**, 30 (1999).

[19] M. Biyajima, M. Ide, M. Kaneyama, T. Mizoguchi, and N. Suzuki, Prog. Theor. Phys. Suppl. **153**, 344 (2004).

[20] A. Bialas and W. Czyz, Acta Phys. Polon. B **36**, 905 (2005).

[21] B.B. Back, et al., Phys. Rev. Lett. **93**, 082301 (2004).

[22] F. James, CERN Report 81-03 (1981).

Table 1. Produced charged hadrons as functions of centrality in d + Au collisions at $\sqrt{s_{NN}} = 200$ GeV, $y_b = \pm$ 5.36 in the Relativistic Diffusion Model. The average impact parameter for each centrality bin is $< b >$, the corresponding equilibrium value of the rapidity is y_{eq}, the variance of the central source in $y-$space is σ^2_{eq}; $< N_{1,2} >$[1] are the respective average numbers of participants. The number of produced charged particles is $N^{1,2}_{ch}$ for the sources 1 and 2 and N^{eq}_{ch} for the equilibrium source, the percentage of charged particles produced in the thermalized source is n^{eq}_{ch}.

$Centrality(\%)$	$< b > (fm)$	y_{eq}	σ^2_{eq}	$< N_1 >$	$< N_2 >$	N^1_{ch}	N^2_{ch}	N^{eq}_{ch}	$n^{eq}_{ch}(\%)$
0-20	2.53	- 0.944	3.99	13.5	2	131	19	35	19
20-40	4.63	- 0.760	3.95	8.9	1.9	78	17	31	25
40-60	5.99	- 0.564	5.70	5.4	1.7	33	11	38	46
60-80	7.10	- 0.347	7.44	2.9	1.4	9	5	35	71
80-100	8.05	- 0.169	6.89	1.6	1.1	2	2	24	86
min. bias	5.66	- 0.664	4.04	6.6	1.7	56	15	21	23

Figure captions

Fig. 1 Time evolution of the analytical solutions in the three-sources Relativistic Diffusion Model (RDM) for minimum-bias d + Au collisions at $\sqrt{s_{NN}}$ = 200 GeV. The curves in the upper frame show the three partial pseudorapidity distributions $(dN_{ch}/d\eta)_k$ and their incoherent sum at short times $\tau_{int}/\tau_y = 0.005$ corresponding to p=0.01. In the lower frame, $\tau_{int}/\tau_y = 2.3$ corresponding to p=0.99 displays the solutions for large times where they come close to statistical equilibrium. Strong interaction stops long before this situation is reached, see Fig.2.

Fig. 2 Calculated pseudorapidity distributions of charged hadrons in d + Au collisions at $\sqrt{s_{NN}}$ = 200 GeV for five different collision centralities, and minimum-bias in comparison with PHOBOS data [1, 21]. The analytical RDM-solutions are optimized in a fit to the data. The corresponding minimum χ^2-values (top left to bottom right) are 4.7, 5.9, 2.4, 1.7, 1.9, 2.1. Au-like, d-like, and central partial distributions are shown for each centrality. Only the midrapidity part comes close to local equilibrium.

Fig. 3 Calculated pseudorapidity distributions of charged particles from d + Au collisions at $\sqrt{s_{NN}}$ = 200 GeV for five different collision centralities, and minimum-bias in comparison with PHOBOS data [1, 21]. The steeper slope in the deuteron direction is due to the nonequilibrium properties of the system.

Fig. 4 Time evolution of the analytical solutions in the three-sources Relativistic Diffusion Model (RDM) as in Fig.1, but for central (0-6%) Au + Au collisions at $\sqrt{s_{NN}}$ = 200 GeV. The curves in the middle frame show the three partial pseudorapidity distributions at short times $\tau_{int}/\tau_y = 0.005$ corresponding to p=0.01. In the lower frame, the distributions are close to equilibrium with $\tau_{int}/\tau_y = 2.3$ (p=0.99). The upper frame gives the comparison with PHOBOS data [3]; here, $\tau_{int}/\tau_y = 0.46$ (p=0.6).

Fig. 5 Calculated pseudorapidity distributions of charged hadrons in Au + Au collisions at $\sqrt{s_{NN}}$ = 200 GeV for six different collision centralities in comparison with PHOBOS data [2, 3]. The relative strength of the midrapidity source at each centrality is chosen here in analogy to d + Au, cf. text. The analytical RDM-solutions are optimized in a fit to the data. The corresponding minimum χ^2-values (top left to bottom right) are 1.2, 1.0, 0.95, 0.67, 0.53, 0.70. Only the midrapidity part comes close to local equilibrium. Its relative importance increases with decreasing centrality.

$p = 0.01$

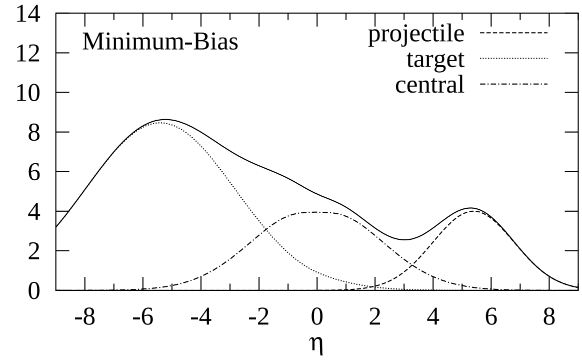

Minimum-Bias
projectile
target
central
η

$p = 0.99$

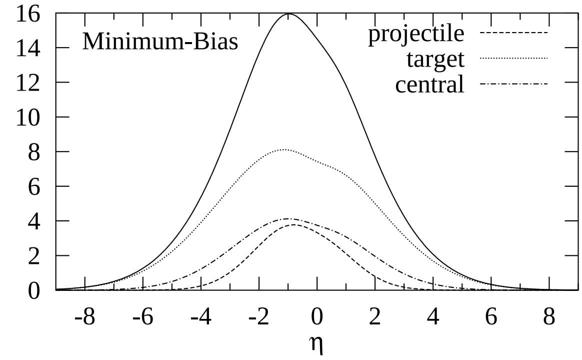

Minimum-Bias
projectile
target
central
η

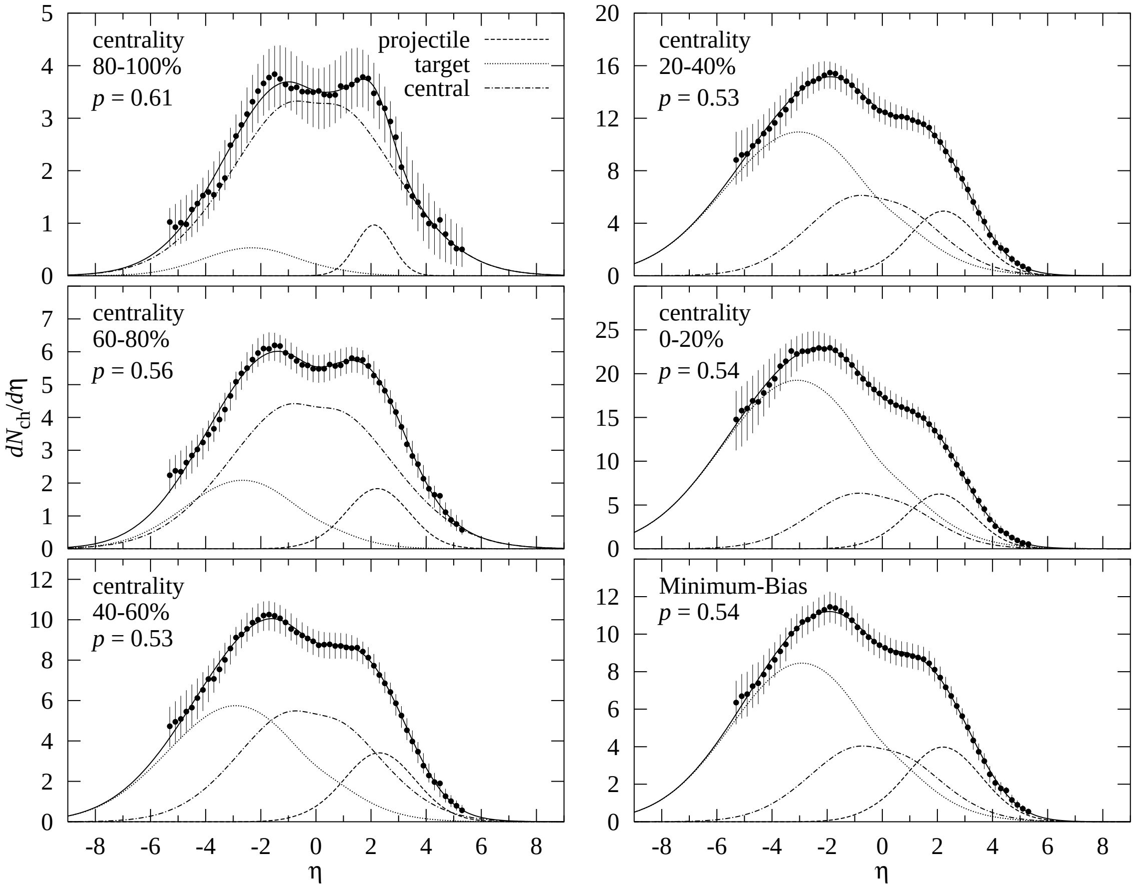

centrality
80-100%
p = 0.61
projectile
target
central
centrality
20-40%
p = 0.53
centrality
60-80%
p = 0.56
centrality
0-20%
p = 0.54
centrality
40-60%
p = 0.53
Minimum-Bias
p = 0.54
$dN_{ch}/d\eta$
η

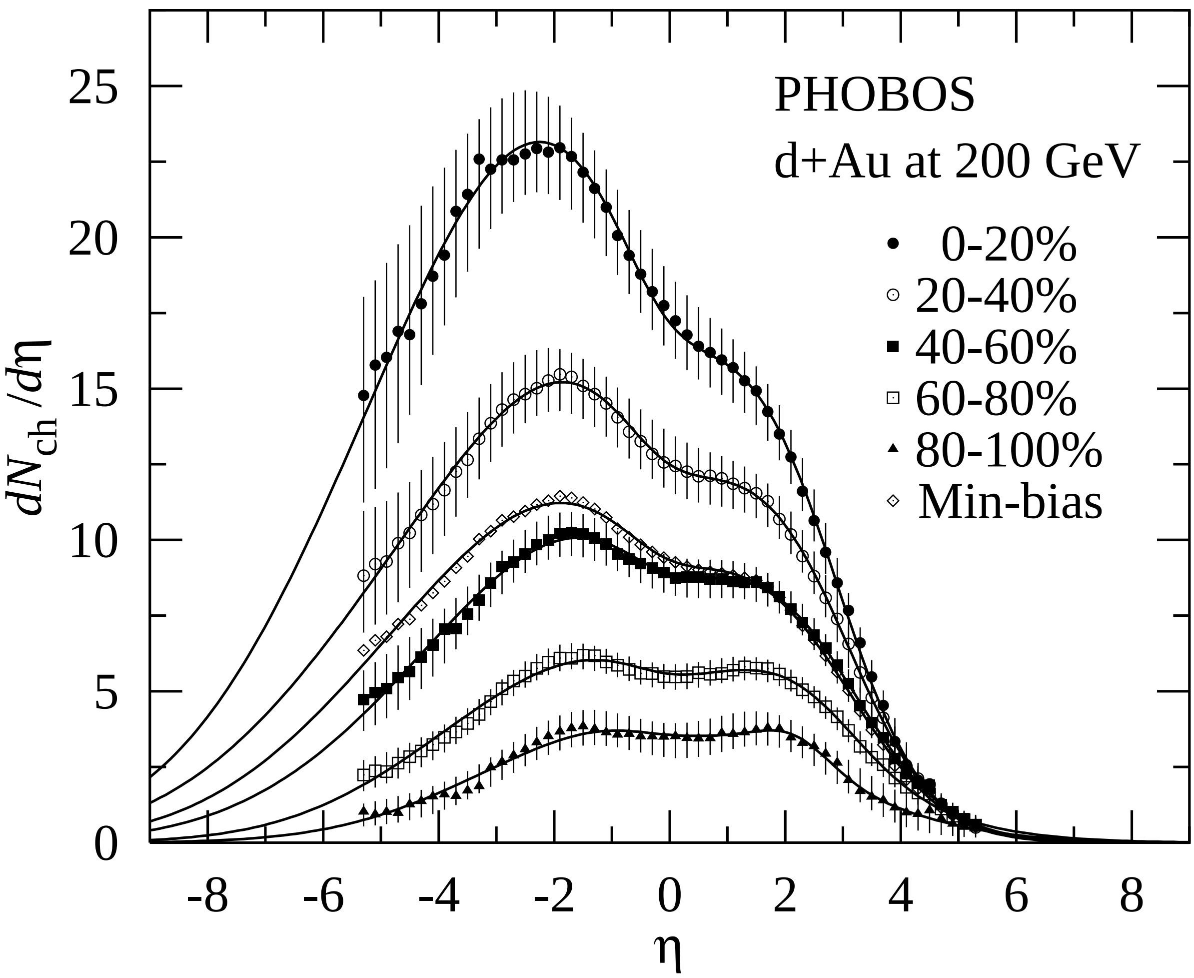

PHOBOS
d+Au at 200 GeV
0-20%
20-40%
40-60%
60-80%
80-100%
Min-bias
$dN_{\rm ch}/d\eta$
η
25
20
15
10
5
0
-8
-6
-4
-2
0
2
4
6
8

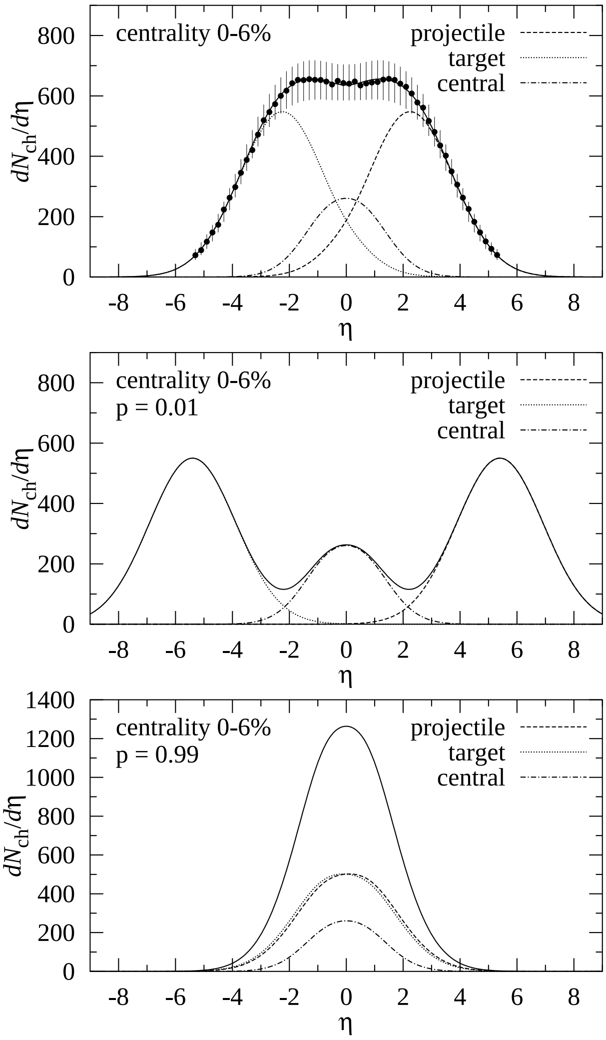
centrality 0-6%
projectile
target
central
$dN_{ch}/d\eta$
η
centrality 0-6%
p = 0.01
projectile
target
central
$dN_{ch}/d\eta$
η
centrality 0-6%
p = 0.99
projectile
target
central
$dN_{ch}/d\eta$
η

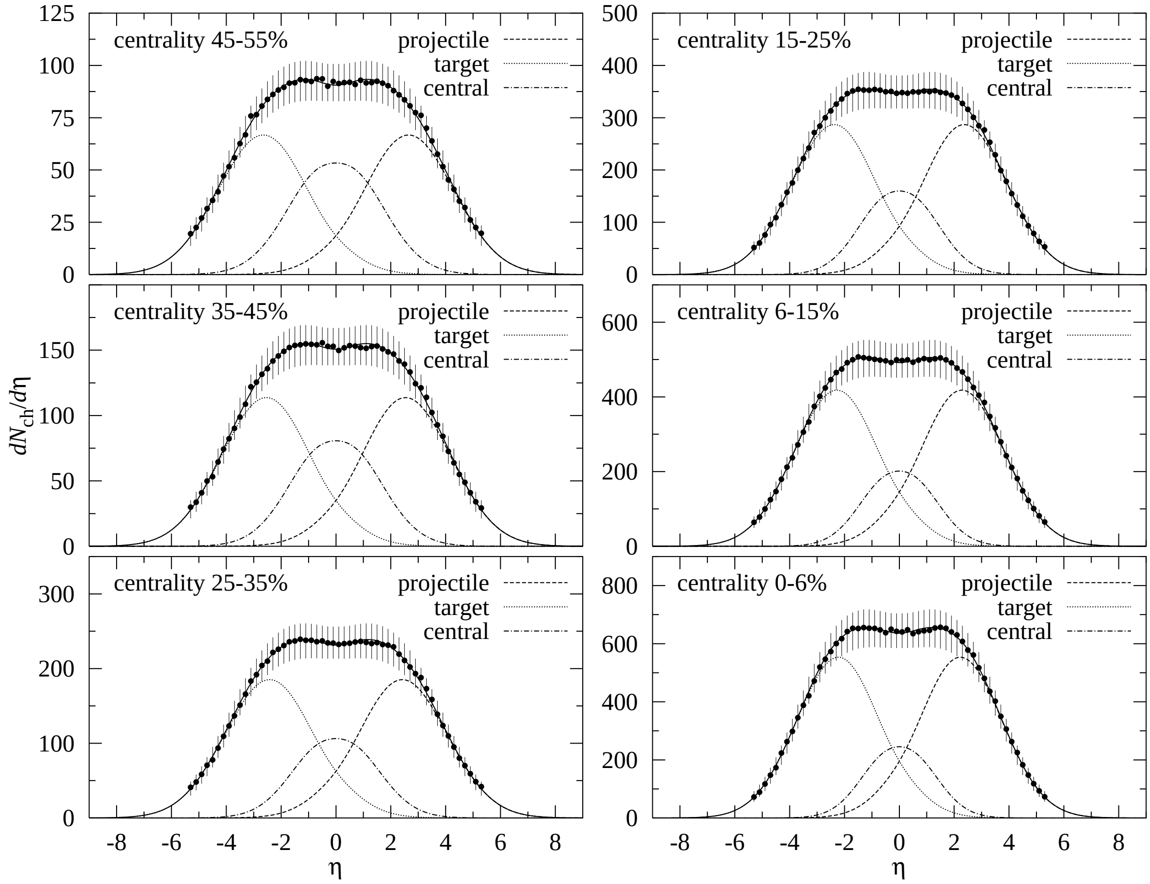
centrality 45-55%
centrality 15-25%
centrality 35-45%
centrality 6-15%
centrality 25-35%
centrality 0-6%
projectile
target
central
$dN_{ch}/d\eta$
η